Single-exposure Volumetric Holographic Additive Manufacturing

Dajun Lin[1], Xiaofeng Chen[2], Connor O'Dea[2], Kwon Sang Lee[3], Apratim Majumder[1], Michael Cullinan[3], Chih-Hao Chang[3], Zachariah A. Page[2], Rajesh Menon[1,4*]

[1]*Department of Electrical and Computer Engineering, University of Utah, Salt Lake City, UT 84102, USA*

[2]*Department of Chemistry, The University of Texas at Austin, Austin, Texas 78712, USA*

[3]*Walker Department of Mechanical Engineering, University of Texas at Austin, Austin, TX 78712, USA*

[4]*Oblate Optics, Inc. San Diego CA 92130, USA*

Corresponding author: rmenon@eng.utah.edu

Abstract: We demonstrate a novel method for single-exposure volumetric additive manufacturing of arbitrary three-dimensional (3D) microstructures. Arbitrary 3D geometries of light can be generated via a holographic mask through inverse design. Such geometries can be simultaneously polymerized within UV resin. We additionally demonstrate and experimentally validate a convolution-based model for detailed printing condition analysis.

Introduction: Creating 3D printed objects typically involves additive techniques, building layers from a digital file. Traditional 3D nanofabrication uses a bottom-up approach, limited by point-build construction, with speed influenced by resolution, layer count, and material polymerization. Here, we experimentally demonstrate a novel method to improve fabrication efficiency by enabling the use of a single phase mask that generates an entire 3D structure, as illustrated shown in Fig. 1(a). The phase mask is a computer-generated hologram (CGH), which can be inverse-designed using the TensorFlow framework and fabricated via grayscale optical lithography (DWL 66+, Heidelberg) in positive-tone photoresist S1813. For UV printing, a mixed resin comprising 0.6 mol/m³ Phenylbis (2,4,6-trimethylbenzoyl) phosphine oxide and 100 wt% Di-pentaerythritol pentaacrylate (Sigma Aldrich, USA) is utilized.

The printing results of hollow cylinder and hollow cubes after development and rinsing are shown in Fig. 1(c). The prints exhibit good quality and agreement with the intended designs. It is worth noting that the prints have rounded corners, which result from radical diffusion. To investigate this effect further, we tested the diffusion range of a voxel generated by the focal point of a convex lens within a thin resin layer under varying exposure times and doses. The experimentally characterized diffusion range, presented in Fig. 1(d), shows a nonlinear trend across different power levels. Notably, the slope of the diffusion range curve greatly decreases as the power approaches the polymerization threshold.

To model this behavior, we developed a convolution model with multi-level kernel sizes based on pattern intensity to simulate diffusion during actual printing, as illustrated in Fig. 1(e). Additionally, Fig. 1(f) presents two examples of failed 3D prints, highlighting issues such as over-curing and the formation of unintended structures outside the main design. In conclusion, the multi-level kernel convolution model provides a robust interpretation of the printing results. With appropriate printing conditions, single-exposure volumetric additive manufacturing of a 3D object can be successfully achieved.

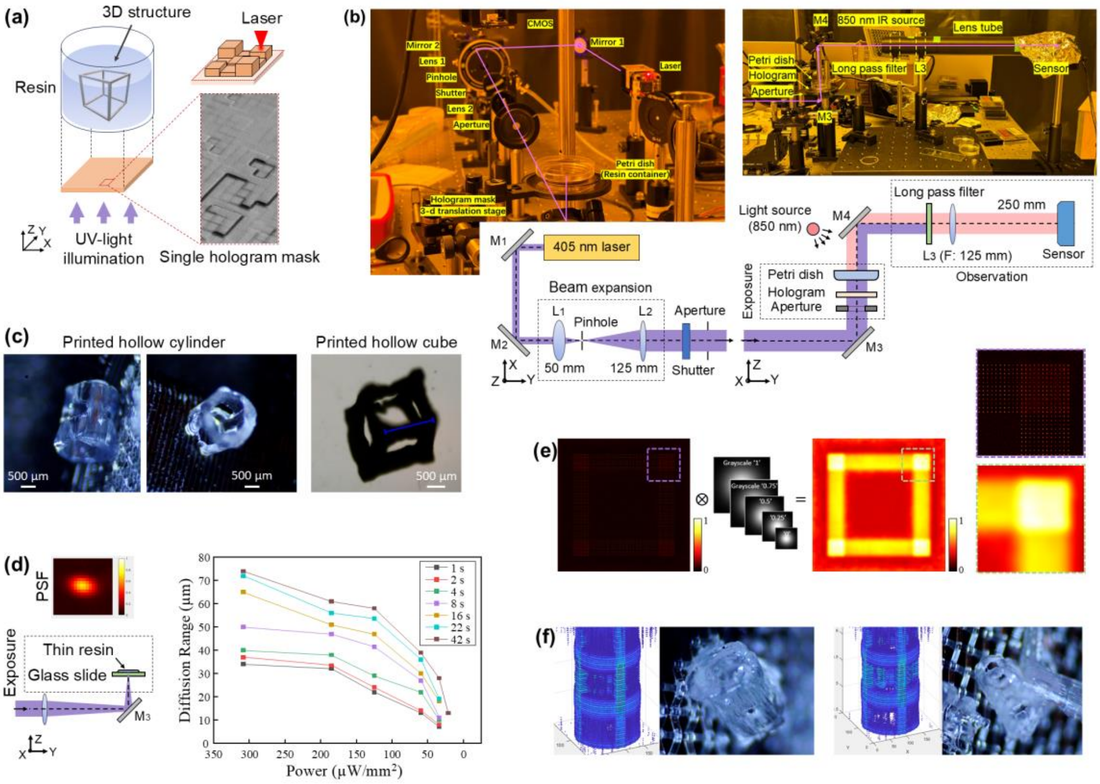

Figure 1. Illustration of the single-exposure holographic additive manufacturing. (a) A phase mask is used to generate a 3D object. The mask is 2.4 mm × 2.4 mm with minimum feature size of 2 μm. (b) Optical setup for printing, including laser collimation, beam expansion, exposure, and observation system. (c) Printing results of the hollow cylinder, and hollow cube. The 3D structures have dimensions of 1.8 mm × 1.8 mm × 1.8 mm, with smallest rod widths of 300 μm. (d) A 50-mm lens is used for diffusion measurement, with a focal size of 6 μm and beam area of 34 μm^2. The plot shows the diffusion range of the foci under varying laser power and exposure time. (e) The experimental data based multi-level kernel size convolution model is utilized to simulate the actual printing. (f) The comparison of simulation results and experimental results. The left model is segmented with a lower threshold, illustrating an over-cured structure. The right model shows multiple unintended windows outside the main structure.